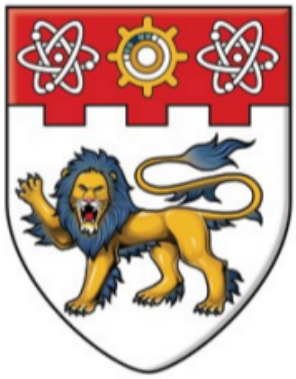

NANYANG TECHNOLOGICAL UNIVERSITY

CONTACT FORCE ESTIMATION USING MOTOR CURRENTS OR TORQUES

RAYMOND DJAJALAKSANA

SCHOOL OF MECHANICAL ENGINEERING

2015/2016

NANYANG TECHNOLOGICAL UNIVERSITY

C014
CONTACT FORCE ESTIMATION USING MOTOR CURRENTS OR TORQUES

Submitted in Partial Fulfillment of the Requirements
for the Degree of Bachelor of Mechanical Engineering
of the Nanyang Technological University

by

RAYMOND DJAJALAKSANA

SCHOOL OF MECHANICAL ENGINEERING
2015/2016

Abstract

The abstract is a highly condensed version of the whole project. Its function is to draw the reader's attention to the main points or findings of the project. It should include: (a) (b) (c) (d) (e) A concise statement of the problem investigated, hardware to be designed, or software to be written Purpose of the project A concise description of how the information was collected, the design methodology or the software approach used in the project The results A concise summary of conclusions and recommendations. The ordering of the above varies according to the type of readers and the purpose of the report. The general rule is to start with information that is most important or interesting. This part of the report should be written only after the whole report is completed and not before. The abstract can be broken up into a small number of paragraphs but the length is usually limited to one A4 page. Single line spacing is allowed in the Abstract.

Acknowledgments

I would like to express my sincere gratitude and appreciation to the following people for their generous help and guidance, which made this final year project become feasible, enjoyable, and fruitful.

Assistant Professor Pham Quang Cuong, the project supervisor, for being generous with his advices and guidance.

Mr Fransisco Surez, the research fellow, for his continuous help and assistance during the whole completion of the project.

All members of CRI group, for their invaluable support regarding project matters.

Contents

List of Tables

List of Figures

Chapter 1

Introduction

1.1 General Introduction

Nowadays, robotics play a very crucial role in industrial area by greatly increasing the industrial productivity. It helps factory workers on doing many monotonous and tedious taks such as pick and place and welding operation. However, this achievement is done because of a highly structured environment such as heavy industry (for example car assembly) where every parameters are known and fixed. In contrast, robotics performance in light industry are still poor. For instances, assembly of small and fragile parts in electronics, food, and other industries. This is because robotics are still bad in dealing with dynamics and unstructured environment where uncertainities are common.

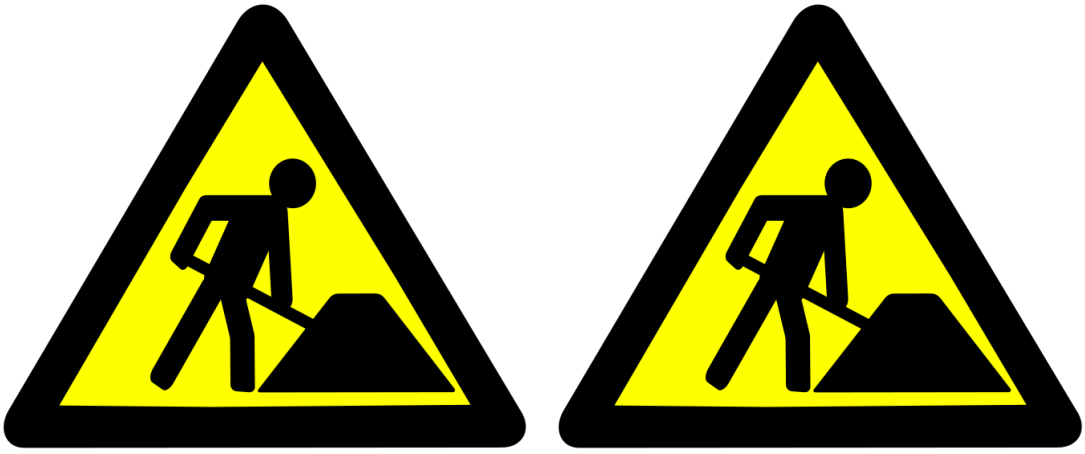

(a) Robotics in heavy industries (b) Manipulators for assembly task

Figure 1.1: Robotics in some applications

In light of this, researches and developments in this topic are still intense

until now. Many works have attempted to create a framework for fine assembly procedures. Recently, a paper by (?, ?) has introduced the complete framework for fine assembly task. However, there are still lots of improvement that can be done.

For robotic assembly task, the robotic arm must be able to cooperate with a lot of uncertainites in the dynamic environment. One example, the manipulator has to be able to know when the contact with an object is happening and then maintaining the stable contact throughout the task. This ability requires knowledge of contact force for the robot. Thus, estimation of contact forces is very important since it will help the robot to determine and control the contact with objects in dynamics environment. While this can be done using accurate force/torque sensor, the sensor is normally expensive and requires mechanical integration with the robotic arm (Wahrburg, Morara, Cesari, Matthias, & Ding, 2015). Hence in some arms it might not be possible to attach this sensor.

In regards to this, many researches have been done in order to estimate the contact force. The main idea to estimate the contact force is to directly apply dynamic equations of a robot, knowing the value of joint torques. However different approaches have also been explored in the past few decades. Early approaches use observers for force estimation like in (Ohishi, Miyazaki, Fujita, & Ogino, 1991). Another approach in (Stolt, Linderoth, Robertsson, & Johansson, 2012) involves detune the low-level joint position control loop to estimate contact force. Furthermore, recent approaches by using Bayesian approach and generalized momentum with Kalman filter are studied in (Wahrburg, Zeiss, Matthias, & Ding, 2014) and (Wahrburg et al., 2015) respectively. Additionally, studies of comparison between two different approaches are done in (Damme et al., 2011). The study compares the result from filtered dynamic equation of external force with generalized momentum method.

1.2 Objective

This project aims to estimate the contact force of an assembly robot based on the arm motor currents/torques. Understanding of the mathematical model of the robots dynamic, friction, and control theory are considered as important knowledge to work with this project.

The project will be focusing on a certain Denso arm. Thus, the developed systems will be built specifically for this arm. Additionally, some problems that are discussed in this project will be only addressed for this Denso arm and might

not be available for other arms.

1.3 Scope

The scope of this project is divided into four parts. First, the project will start from understanding of the general models of robot dynamic and friction. Thus, literature reviews and readings are included in this step. The next step is to perform some experiments to get all necessary data to develop the model. This includes setup preparations, running the experiments, and collections of the data. The third step will be processing all the results and develop the system to estimate the contact force. which after that, validation of the built model to the real data will be the final step.

Chapter 2

Literature Review

2.1 Background

2.2 Purpose and scope

1	2	3
4	5	6
7	8	9

Table 2.1: A simple table

Figure 2.1: NTU logo

First eref (Wahrburg et al., 2014) asdfsdf

Second (Damme et al., 2011) asfdasdf

Third (Bona & Indri, 2005) asfdsf

fourth (Ohishi et al., 1991)

Chapter 3

Mathematical Model

3.1 Arm Dynamic Equation

The basic dynamic equation of a six degrees of freedom (6-DOF) robotic arm is described by:

$$\Sigma\tau_{joint} = \tau_{mot} + \tau_{ext} = M(q)\ddot{q} + C(\dot{q}, q)\dot{q} + G(q) + \tau_{friction} \tag{3.1}$$

Where τ_{mot} is the motor torque, τ_{ext} is the external wrench / torque applied to the respective joint where in this project is due to end-effector force / torque, and $\tau_{friction}$ is the torque because of joint friction. $M(q)$ defines the inertia matrix, $C(\dot{q}, q)$ defines the coriolis matrix, and $G(q)$ is the joint torque resulting from gravity. In other words, for each of joint, the summation of external joint torques ($\tau_{mot} + \tau_{ext}$) are equal to the torques needed to overcome the friction and to perform the dynamic motion. Initially the motor torque will be calculated from motor currents by using the relation:

$$\tau_{mot} = K_m I_{mot} \tag{3.2}$$

However, there is a problem regarding motor currents where the solution is to get the motor torque value directly from the arm (see chapter 5.1). And since the unit is in percentage (%) and not in SI unit, calibration is needed to change it to SI. Thus, it can be written as:

$$\tau_{mot} = K_{denso}\tau_{denso} \tag{3.3}$$

Where K_{denso} will be called denso gain for ease of reference.

On the other hand, transformation of the end-effector force/torque to the joint wrench, the jacobian matrix is needed, which the equation is:

$$\tau_{ext} = J^T F_{ext} \tag{3.4}$$

Where $J^T \in R^{6\times6}$ is the transpose of jacobian matrix and $F_{ext} = [F\ \tau] \in R^{6\times1}$ is the contact force. It is also important to consider friction since it can cause large error in manipulators (?, ?). However, the modeling of friction is not easy as there are a lot of phenomenas in the friction itself. Thus, it is good to choose the simplest model that can have a reasonable result. The next section below will explain the friction model in more detail.

3.2 Friction Model

In general, friction models can be divided into two categories: static and dynamic friction. A model that depends only on current velocity is called static friction, whereas the friction related to non-stationary velocities is called dynamic model.

In static friction, including coulomb and viscous friction, stiction phase and stribeck effect can be also captured. However, dynamic friction can capture more phenomenas such as: small displacements occurring during stiction phase, hysteretic effect, and variations in break-away force. In short, dynamic model explains the friction in microscopic level and hence can capture more phenomenas.

During the early stage of the project, both type of model will be considered, whereby in the late stage only the static model will be used as dynamic model has some difficulties.

3.2.1 Static Friction Model

Viscous and Coulomb is the simplest form of static friction model. The basic mathematical form is as below:

$$F = F_c sign\,(\dot{x}) + \beta\dot{x} \tag{3.5}$$

Where F is the friction force, ν is relative velocity to contact surfaces, β is the viscous friction coefficient, and F_c is coulomb friction. The model however does not include the stiction effect. The stiction effect can be easily added into the model, that is: a movement can be created only when the applied external force is greater than friction force Fs (Bona & Indri, 2005). By adding this effect and adjusting the equation for robotic arm, the equation will be:

$$\tau_{friction} = K_c sign\left(\dot{q}\right) + K_v \dot{q} \tag{3.6}$$

Because of stiction and coulomb effect, the friction model will introduce discontinuous profile when the direction of velocity changes. The friction force diagram for this model can be seen in figure below where it shows a discontinuity at velocity equals to zero.

Figure 3.1: Static friction profile

3.2.2 Dynamic Friction Model

The well-known Dahl model is the simplest form to describe the dynamic friction behaviour. With Dahl model, hysteretic effects can be explained since it introduces the lag in the changes of friction force as velocity changes. However, Dahl model does not include some other effects, such as stiction and Stribeck effect. A refined form of Dahl model that includes these effects is called LuGre friction model (Bona & Indri, 2005).

Dahl friction plays with an internal state variable z, and then defines the friction force as:

$$\dot{z} = \dot{q} - \frac{|\dot{q}|}{F_c}\sigma z \tag{3.7}$$

$$\tau_{friction} = \sigma z \tag{3.8}$$

Where σ is the bristle stiffness parameter. Because of this internal state z, Dahl model can explain the hysteretic effect in friction. Be aware that for this equation, it requires a correct initial value of z. Figure below shows the diagram of Dahl model.

Figure 3.2: Dahl model of dynamic friction

Unlike Coulomb and viscous friction model, Dahl model does not have discontinuous profile in the equation. This becomes one advantage Dahl model has over the static friction. However, since the model is more complex, it imposes some difficulties such as: estimation of initial state is not easy, it is sensitive to the parameter (σ), and the necessity of high precision data.

Chapter 4

Equipments

In this project, necessary equipments, software, and robotic arm that are going to be used are: 1 × Denso VS060A3-AV6 arm, 1 × end-effector handle, 1 × ATI Gamma F/T Sensor (SI-32-2.5 calibration), Ubuntu 12.04 LTS, OpenRave, and Denso ROS.

4.1 Denso VS060

Denso VS060A3-AV6 is a six DOF robotic arm from Denso company. It has absolute encoder for all of its joint position. An RC-8 controller is also provided for interfacing with this arm. The computer is connected to Denso arm via LAN cable. The architecture of the hardware interface for this arm can be seen in figure below.

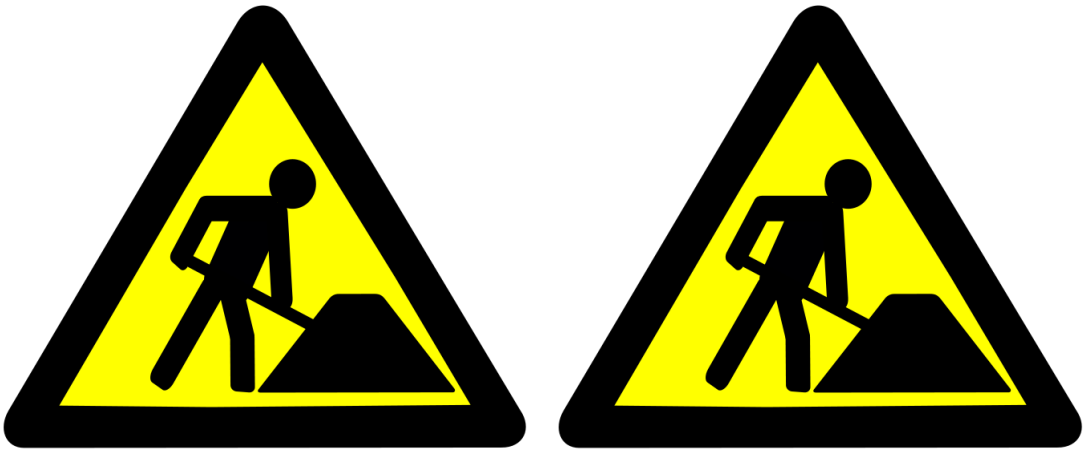

(a) Denso VS060 arm (b) Hardware interface of Denso arm

Figure 4.1: Denso VS060A3-AV6

4.2 ATI Gamma F/T Sensor

This F/T Sensor is attached into the end-effector of Denso arm to measure the contact force and torque. After this sensor, another handle is attached on top of the F/T sensor. Hence, with the addition of contact force and torque, F/T sensor will also read the weight and inertial force from the handle.

Figure 4.2: ATI Gamma F/T Sensor

4.3 End-effector handle

This is the handle of the end-effector arm. It has a round sphere surface. The arm will make a contact with environments through this handle.

Figure 4.3: End-effector handle

4.4 Ubuntu 12.04 LTS

The OS of the working computer is Linux Ubuntu, with version of 12.04. It is not the lattest version and it should stay in 12.04 version for operating the arm.

Some important packages are also installed, they are OpenRave and Denso ROS. Python and C++ are used to run the Denso arm.

4.5 OpenRave

OpenRAVE is a package that provides an environment for testing, developing, and deploying motion planning algorithms in robotics applications. It focuses on the simulation analysis of motion planning. It is to be used together with Denso ROS to control the Denso arm with its analysis guidance. The OpenRave is oftenly used in Python script.

Figure 4.4: OpenRave environment

4.6 Denso ROS

Denso ROS is a robot operating system that works on the Denso arm. With Denso ROS, the manipulator arm can be controlled from computer. The packages are written in C++ and Python while the script to run the robot is usually written in Python codes.

Chapter 5

Methodology

5.1 Motor Currents Reading

Before continue with more experiment and identification, there is one problem that needs to be solved first. The problem is that the arm only gives absolute value of the motor currents (Fig. 5.1a). Thus there is a need to identify the sign of the motor currents of each joints. Three methods were tried but only one was successful.

The first attempt was to give the motor current sign based on the sign of τ_{dyn} during non-contact condition. However, this poses a problem when the τ_{dyn} goes near zero as it will not be clear enough to identify the sign. The second method was to match the derivative of motor currents with derivative τ_{dyn} during pre-contact motion (e.g.: if τ_{dyn} is increasing, the motor currents has to be increasing too, and vice versa). Unfortunately, this principle working only if motor currents are very smooth and steady which is a very difficult condition.

After the first two attempts, it was found out that we can actually extract motor torques value from Denso and this time it includes the sign of it. The data is then plotted against motor currents with the sign of motor torques to see the relation. From Fig. 5.2 we can see that there is a good linearity between these two variables, and so we can now actually use motor torques instead of motor currents. By doing this, not only we do not need to take care of the currents sign problem anymore, we also simplify our problem since what we are interested in is the motor torques, not motor currents. However, since the value is not in the SI unit calibration is needed to adjust the value into the SI unit.

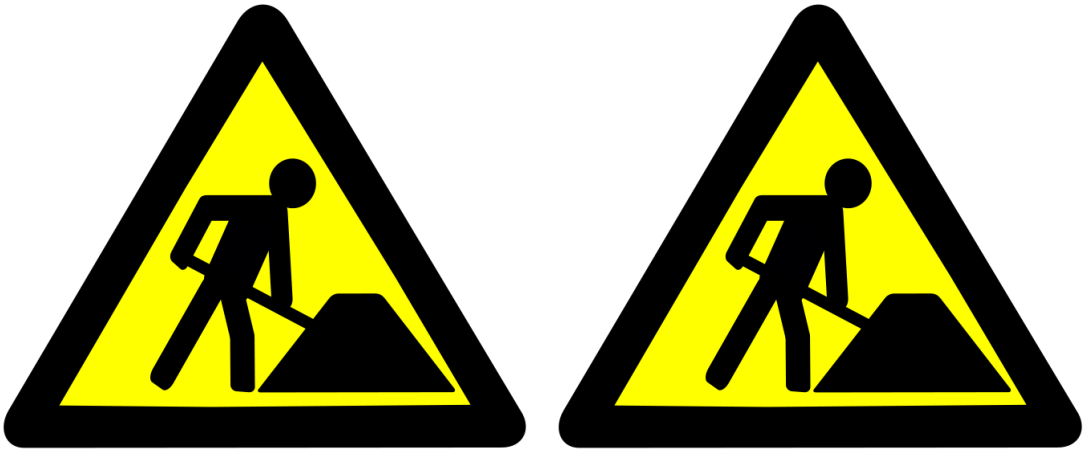

(a) Raw data of motor currents (b) Raw data of motor torques

Figure 5.1: Reading of motor currents

Figure 5.2: Motor torques vs motor currents with sign

5.2 Two-Stage Experiment

There are two stage of experiments which are required to identify the two important parameters : K_{denso} and $\tau_{friction}$ (see chapter 3.1). The purpose of setting different type of experiment is to eliminate the effect of other parameter, thus the resulted data is affected only because of one parameter. That way the identification of each parameter tends to be easier and more accurate. The first stage of experiment is the high torque collection data to calibrate the motor torque (K_{denso}) while the second stage of experiment is the high velocity collection data which is performed to identify the $\tau_{friciton}$ characteristics. The data is captured in broad range of value to capture as many phenomena as possible.

5.2.1 High Torque Collection Data

The experiment is meant to collect the torque measurement from wide range to calibrate the motor torque. Firstly, the robot is moved to a position where the interested joint will receive a high torque from contact force. While the robot is fixed, the force is introduced at the end-effector of the arm such that the interested joint will experience a high torque. Motor torques are recorded from Denso arm and contact force/torque are recorded through ATI F/T sensor. The experiment is repeated in a different position for each joints. See figure below for illustration.

Figure 5.3: High torque collection data experiment

5.2.2 High Velocity Collection Data

For this second experiment, the robot is moving in a free motion. Thus, a free rotation with different velocity is performed for each of respective joints. In this way, the effect of friction can be clearly caprtured. Motor torques, and joint positions which are crucial parameters are recorded from Denso manipulator for further analysis. See figure below for illustration.

Figure 5.4: High velocity data experiment

Chapter 6

Results and Model Identification

6.1 Preliminary Results

Two figures below are some samples of the collected data during the experiment. The whole data are available in the *APPENDIX*. The data has been filtered to eliminate the noise reading available from the sensor or motor. It uses low pass filter for smoothing the result. Low pass filter for F/T sensor have the order of 3 with cutoff frequency of 2 Hz. As for the motor torque, the low pass filter is set to have the order of 5 and cutoff frequency of 1 Hz.

Fig. 6.1 represents the result of high torque experiment for one of the joint and Fig. 6.2 represents the data collected during the free motion experiment. The results from Fig. 6.1 will be further processed for calibrating the motor torque while results in Fig. 6.2 are used for friction identification.

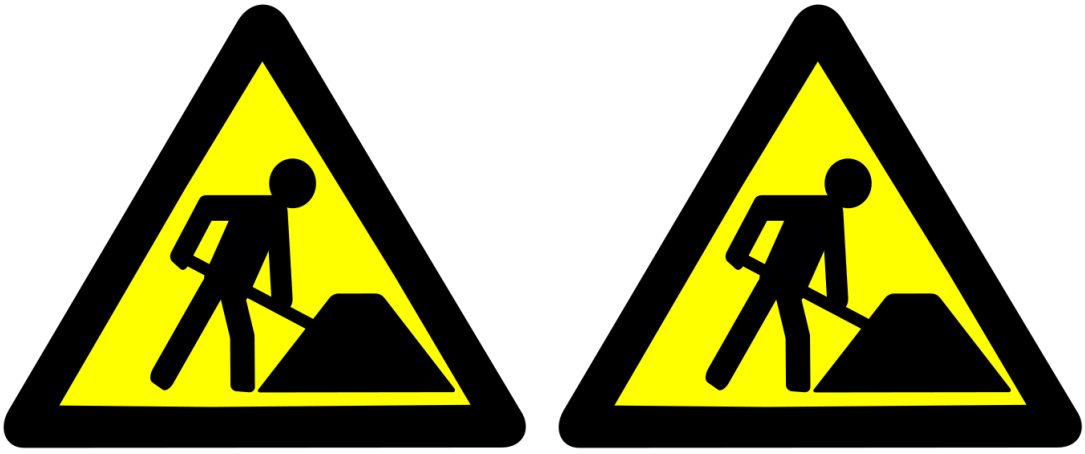

(a) Filtered data of external wrench detected from F/T sensor

(b) Filtered data of motor torques

Figure 6.1: Sample data of the second joint high torque experiment

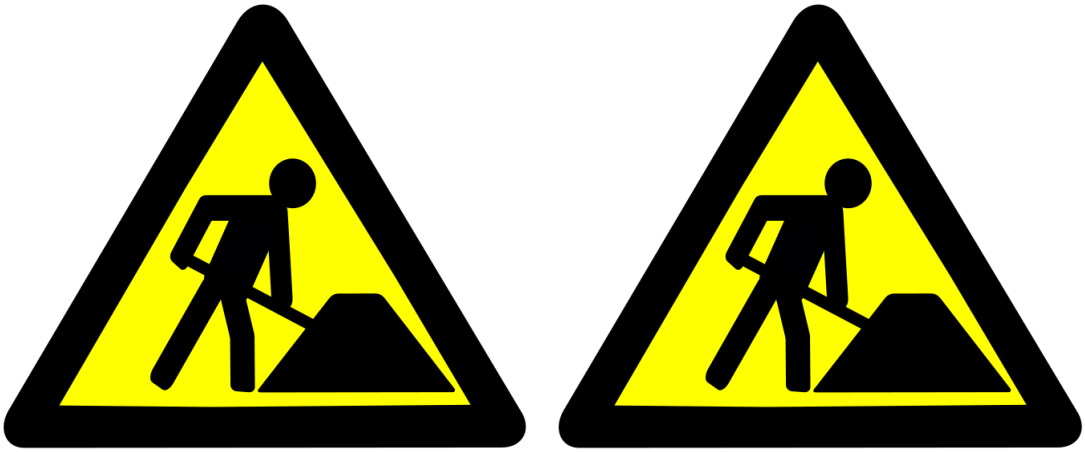

(a) Calculated joint torque using OpenRave (b) Filtered data of motor torques

Figure 6.2: Sample data of the second joint high velocity experiment

6.2 Motor Torque Calibration

6.2.1 Motor Torque Gain Identification

Based on the setup that has been mentioned in subsection 5.2.1, it is known that during the experiment the joints are stationary and hence $\dot{q} = 0$, $\ddot{q} = 0$. Also since it is not moving, there is no friction effect for the joint. And by using relation in (3.3) and (3.4), equation (3.1) can be simplified to:

$$K_{denso}\tau_{denso} + J^T F_{ext} = G\left(q\right) \tag{6.1}$$

Taking the reference value when there is no external wrench (at $F_{ext} = 0$), the above equation becomes:

$$K_{denso}\tau'_{denso} = -J^T F_{ext} \tag{6.2}$$

This makes the calibration of K_{denso} becomes more easier to identify as it is a simple linear problem. To get the value of K_{denso}, the model is optimized from the data (τ'_{denso}, F_{ext}) that has been gathered. The optimization is done using nelder-mead method.

The diagram in Fig. 6.3 shows the plot of τ'_{denso} against $-J^T F_{ext}$. The red dots represent the experimental data while the black line is the model with optimized parameter K_{denso}. As it can be seen, the data is not perfectly linear as what it is supposed to. The nonlinearity especially happens around zero value. The reason

might be because of the deadzone in motor controller: where errors below some value will be counted as zero.

Figure 6.3: τ'_{denso} vs $-J^T F_{ext}$ in high torque experiment for second joint

6.2.2 Verification of Motor Torque Calibration

To verify the value of K_{denso}, a simple setup experiment can be done. The setup can be described like this: for one joint, the robot is positioned such that the motor will exert some torque due to the weight of the links only. Because it is not moving and no external force is introduced, the dynamic equation is reduced to be :

$$K_{denso}\tau_{denso} = G(q) \tag{6.3}$$

The value of $G(q)$ is computed using OpenRave. The value should be comparable to the left side of equation.

However, the figure in Fig. 6.4 a different result. The continuous line represents the torque computed from OpenRave, (e.g.:$G(q)$) and the strip line represents the motor torque after calibration (e.g.: $K_{denso}\tau_{denso}$). It is very clear that value is not the similiar. The value given in OpenRave is much higher than motor torque. There are two possibilites that might be the reason of this differences, which are: 1) The gain value (K_{denso}) is incorrect due to some problems that might arise in F/T sensor (i.e.: F/T sensor not calibrated) or 2) The OpenRave gives incorrect computation. It is quite difficult to investigate the second reason as until now the real dynamic parameters of the Denso arm has not been identified, thus torque computation of dynamic motion could not be done for now.

Hence, from this verification it can be found that there are some pieces that are still missing. And so, validation could not be done for now.

Figure 6.4: Joint Torque Verification for Second joint

6.3 Friction Identification

6.3.1 Idenfication of Dahl Model

In the early stage of the progress, Dahl model was chosen as the friction model for the system. The optimization of the model was done to fit with the data. The result is shown in Fig. 6.5. The root-mean-square of the fitting model seem to gives a good result. However, lot of problems were found during the implementation of the model. This comes from the disadvantages of the model itself. Hence, at some stage it is decided to leave the model and change to static friction model which is easier to implement.

Figure 6.5: Fitting of Dahl Model

6.3.2 Static Friction Model

Chapter 7

Model Validations

7.1 Motor Currents Reading

7.2 Purpose and scope

1	2	3
4	5	6
7	8	9

Table 7.1: A simple table

Figure 7.1: NTU logo

First eref (Wahrburg et al., 2014) asdfsdf

Second (Damme et al., 2011) asfdasdf

Third (Bona & Indri, 2005) asfdsf

fourth (Ohishi et al., 1991)

Chapter 8

Conclusion and Future Works

8.1 Background

8.2 Purpose and scope

1	2	3
4	5	6
7	8	9

Table 8.1: A simple table

Figure 8.1: NTU logo

First eref (Wahrburg et al., 2014) asdfsdf

Second (Damme et al., 2011) asfdasdf

Third (Bona & Indri, 2005) asfdsf

fourth (Ohishi et al., 1991)

Wahrburg et al. (2015)

References

Bona, B., & Indri, M. (2005). Friction Compensation in Robotics: an Overview. In *Proc. of 44th ieee conference on decision and control, and the european control conference 2005* (p. 4360-4367).

Damme, M. V., Beyl, P., Vanderborght, B., Grosu, V., Ham, R. V., Vanderniepen, I., et al. (2011). Estimating Robot End-Effector Force from Noisy Actuator Torque Measurements. In *Proc. of ieee international conference on robotics and automation* (p. 1108-1113).

Ohishi, K., Miyazaki, M., Fujita, M., & Ogino, Y. (1991). H observer based force control without force sensor . In *Proc. of industrial electronics, control and instrumentation* (p. 1049-1054).

Stolt, A., Linderoth, M., Robertsson, A., & Johansson, R. (2012). Force Controlled Robotic Assembly without a Force Sensor. In *Proc. of ieee international conference on robotics and automation* (p. 1538-1543).

Wahrburg, A., Morara, E., Cesari, G., Matthias, B., & Ding, H. (2015). Cartesian Contact Force Estimation for Robotic Manipulators using Kalman Filters and Generalized Momentum. In *Proc. of ieee international conference on automation science and engineering* (p. 1230-1235).

Wahrburg, A., Zeiss, S., Matthias, B., & Ding, H. (2014). Contact Force Estimation for Robotic Assembly using Motor Torques. In *Proc. of ieee international conference on automation science and engineering* (p. 1252-1257).